

# Transparency of Magnetized Plasma at the Cyclotron Frequency

G. Shvets

*Illinois Institute of Technology, Chicago, Illinois 60616*

J. S. Wurtele

*Physics Department, University of California, Berkeley, California 94720*

*and Lawrence Berkeley National Laboratory, University of California, Berkeley, California 94720*

(Received 20 February 2002; published 26 August 2002; publisher error corrected 12 September 2002)

Electromagnetic radiation is strongly absorbed by a magnetized plasma if the radiation frequency equals the cyclotron frequency of plasma electrons. It is demonstrated that absorption can be completely canceled in the presence of a magnetostatic field of an undulator, or a second radiation beam, resulting in plasma transparency at the cyclotron frequency. This effect is reminiscent of the electromagnetically induced transparency (EIT) of three-level atomic systems, except that it occurs in a completely *classical* plasma. Unlike the atomic systems, where all the excited levels required for EIT exist in each atom, this classical EIT requires the excitation of nonlocal plasma oscillation. A Lagrangian description was used to elucidate the physics of the plasma transparency and control of group and phase velocity. This control leads to applications for electromagnetic pulse compression and electron/ion acceleration.

DOI: 10.1103/PhysRevLett.89.115003

PACS numbers: 52.35.Hr, 42.25.Bs, 52.35.Mw, 52.38.Kd

Electromagnetically induced transparency (EIT) in quantum-mechanical atomic systems is a well understood and thoroughly studied [1] subject. EIT is the basis of several applications, such as slow light [2] and information transfer between matter and light [3]. Several recent reviews [4] elucidated the quantum-mechanical mechanism of EIT, which relies on the destructive interference between several pathways connecting the ground and excited states of the atom. This Letter presents the physics of induced transparency and reduced group velocity in a classical plasma and proposes applications to accelerators and energy compression.

We consider an externally magnetized plasma with  $\vec{B} = B_0 \vec{e}_z$  and density  $n_0$ . A right-hand polarized electromagnetic wave (probe) at a frequency  $\omega_1$  equal to cyclotron frequency  $\Omega_0 = eB_0/mc$  cannot propagate in the plasma because it undergoes resonant cyclotron absorption [5]. The cold magnetized plasma dispersion relation  $\omega_1$  vs  $k_1$  for the right-hand polarized probe, plotted in Fig. 1, is given by  $\omega_1^2 = k_1^2 c^2 + [(\omega_p^2 \omega_1)/(\omega_1 - \Omega_0)]$ . A band gap develops between  $\Omega_0$  and  $\Omega_{RH} = \sqrt{\Omega_0^2/4 + \omega_p^2} + \Omega_0/2$ , where  $\omega_p = (4\pi e^2 n_0/m)^{1/2}$ . Transparency is achieved by adding a second intense electromagnetic wave (pump) with frequency  $\omega_0 = \Omega_0 - \omega_p$ . Moreover, if  $\omega_p = \Omega_0$ , a magnetostatic undulator makes plasma transparent.

The mechanism of classical electromagnetically induced transparency is the destructive interference between the electric field of the probe ( $\vec{E}_{1\perp}$ ) and the sidebands of the electric ( $\vec{E}_{0\perp}$ ) and magnetic ( $\vec{B}_{0\perp}$ ) fields of the pump. The sidebands are detuned from the pump by  $\omega_p$ , and are produced by the collective electron plasma oscillation along the magnetic field. Qualitatively, the total force at the cyclotron frequency experienced by a plasma electron is given by  $\vec{F}_{\text{tot}} \approx -e(\vec{E}_{1\perp} + \zeta_z \partial_z \vec{E}_{0\perp} + \zeta_z \vec{e}_z \times \vec{B}_{0\perp})$ ,

where  $\zeta_z$  is the electron displacement in the plasma wave. With the probe alone, the resonant  $\vec{E}_{1\perp}$  generates an induced plasma current that dominates the displacement current and prevents wave propagation. With both the pump and probe, and the amplitudes and phases of the electromagnetic and plasma waves properly correlated, the net force can vanish ( $\vec{F}_{\text{tot}} \sim 0$ ). Consequently, the plasma current at the cyclotron frequency is small (or even vanishing), and the probe propagates as if in vacuum. Numerical simulation below demonstrates that this correlation is naturally achieved in a collisionless plasma.

We assume two right-hand polarized EM waves propagating along the  $z$  direction, with their electric and magnetic fields given by  $2e\vec{E}_{0\perp}/mc\omega_0 = a_{\text{pump}}\vec{e}_+ \exp(i\theta_0) + \text{c.c.}$ ,  $2e\vec{E}_{1\perp}/mc\omega_1 = a_{\text{probe}}\vec{e}_+ \exp(i\theta_1) + \text{c.c.}$ , and  $\vec{B}_{0,1\perp} =$

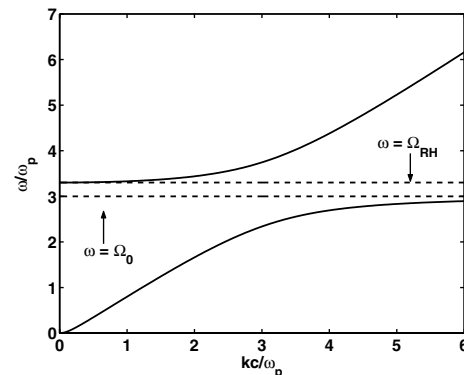


FIG. 1. Dispersion curve for a right-hand polarized wave propagating along a magnetic field. A forbidden gap exists between the cyclotron frequency  $\Omega_0 = eB_0/mc$  and the cutoff frequency of the right-hand polarized wave  $\Omega_{RH} = \Omega_0/2 + \sqrt{\Omega_0^2/4 + \omega_p^2}$ .

$(c\vec{k}_{0,1}/\omega_{0,1}) \times \vec{E}_{0,1\perp}$ , where  $\vec{e}_\pm = \vec{e}_x \pm i\vec{e}_y$ , and  $\vec{\theta}_{0,1} = k_{0,1}z - \omega_{0,1}t$ . The nonrelativistic equation of motion of a plasma electron in the combined fields of the electromagnetic and plasma waves is given by

$$\frac{d^2\vec{x}}{dt^2} + \Omega_0\vec{v} \times \vec{e}_z + \omega_p^2\zeta_z\vec{e}_z = -\frac{e}{m} \sum_{m=0,1} \left( \vec{E}_{m\perp} + \frac{\vec{v} \times \vec{B}_{\perp m}}{c} \right), \quad (1)$$

where  $\vec{x} = (z_0 + \zeta_z)\vec{e}_z + \vec{x}_\perp$  and  $\vec{v} = d\vec{x}/dt \equiv c\vec{\beta}$  are the particle position and velocity. The initial conditions are  $\vec{v} = 0$  and  $\vec{x} = z_0\vec{e}_z$ .

Equation (1) was integrated first with only the probe, and then with both the pump and the probe. The pump and the probe amplitudes were turned on according to

$$\begin{aligned} a_{\text{pump}} &= \frac{a_0}{2} (1 + \tanh[(\Omega_0 t - 160)/40]), \\ a_{\text{probe}} &= \frac{a_1}{2} (1 + \tanh[(\Omega_0 t - 320)/40]). \end{aligned} \quad (2)$$

Simulation results for  $\omega_p/\Omega_0 = 0.3$  ( $\omega_0 = 0.7\Omega_0$ ) are shown in Fig. 2. Without the pump, an electron is resonantly driven by the probe as shown in Fig. 2(a). In the plasma, this growth leads to a large electron current and probe absorption (time averaged,  $\vec{E}_\perp \cdot \vec{v}_\perp < 0$  at the cyclotron resonance,  $\omega_1 = \Omega_0$ ). Adding a strong pump with  $a_0 = 0.1$  and  $k_0 \approx 0.83\Omega_0/c$  dramatically changes electron motion, as seen in Fig. 2(b). After turning on of the pump (but not the probe), an electron oscillates in the field of the pump according to the analytic solution  $\beta_{x0} = \omega_0 a_{\text{pump}}/(\omega_0 - \Omega_0) \sin(k_0 z_0 - \omega_0 t)$ . Switching on the probe does not significantly alter electron motion:  $\beta_x - \beta_{x0}$  appears as a barely visible dashed line in Fig. 2(b). Figures 2(a) and 2(b) illustrate how the pump suppresses electron response at the cyclotron frequency. This suppression results in the plasma transparency at the cyclotron frequency and allows the propagation of the probe.

The suppression of the linear response to the probe is caused by the excitation of a strong plasma oscillation [shown in Fig. 2(c)], which produces a sideband of the pump at the cyclotron frequency. This sideband, in turn, cancels the electric field of the probe. An approximate analytic formula for the steady-state plasma oscillation,

$$\zeta_0 = \frac{2a_{\text{probe}}}{k_0 a_{\text{pump}}} \sin \omega_p t, \quad (3)$$

is derived below by requiring that the sideband cancels the probe. It is in good agreement with the simulation, as seen in Fig. 2(c), where the dashed line shows the difference between the analytic and simulated motion. Simulation results demonstrate the *stability* and *accessibility* of the steady-state values of  $\beta_x$  and  $\zeta_z$  in a collisionless plasma. Note that the pump has to be switched on prior to the arrival of the probe.

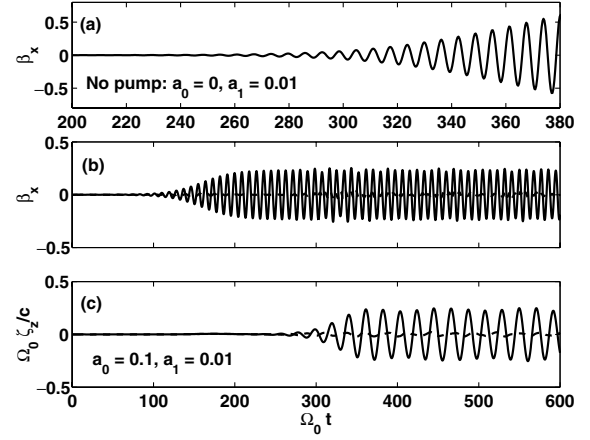


FIG. 2. Numerical simulation of single particle motion in the combined field of two EM waves with  $(\omega_1 = \Omega_0, k_1 = \omega_1/c)$  and  $(\omega_0 = \Omega_0 - \omega_p, \omega_p = 0.3\Omega_0, k_0 \approx 0.83\Omega_0/c)$ . Both the pump and the probe are slowly turned on according to Eq. (2). (a) Without the pump, an electron is resonantly driven by probe:  $\beta_x$  growth indefinitely; (b) With the pump, electron motion is almost unaffected by the probe. Solid line—total  $\beta_x$ ; barely visible dashed line— $(\beta_x - \beta_{x0})$ , where  $\beta_{x0} = \omega_0 a_{\text{pump}}/(\omega_0 - \Omega_0) \sin(k_0 z_0 - \omega_0 t)$  is the analytic result when only the pump is present. (c) Solid line: the longitudinal displacement  $\Omega_0 \zeta_z/c$ ; dashed line:  $\Omega_0(\zeta_z - \zeta_0)/c$ , where  $\zeta_0 = 2a_{\text{pump}}/a_{\text{probe}} \sin \omega_p t$  from Eq. (3).

Generating a high-power pump wave may prove challenging in practice. For example, a dimensionless vector potential of  $a_0 = 0.01$  over an area  $A = (2\pi c/\omega_0)^2$  requires microwave power of the order of 3 MW. Transparency can also be induced by a helical undulator field if  $\omega_p = \Omega_0$ . We simulated electron motion in the combined field of an undulator, with  $a_0 = 0.1$  and  $k_0 = 2\Omega_0/c$ , and a probe, switched on according to  $a_{\text{probe}} = 0.5a_1\{1 + \tanh[(\Omega_0 t - 320)/60]\}$ , where  $a_1 = 0.01$ . Suppression of the electron response at the cyclotron frequency is apparent from Fig. 3(a). The force due to the

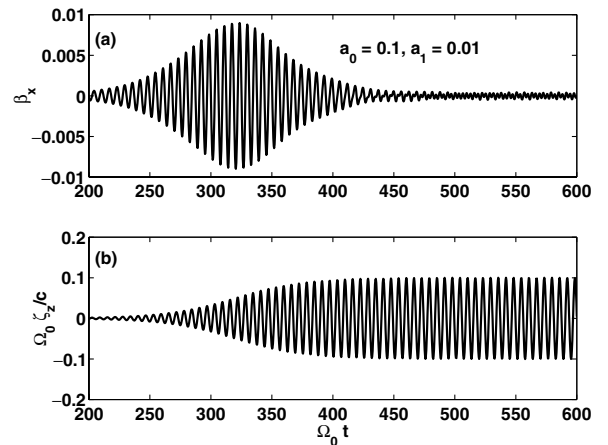


FIG. 3. The same parameters as Fig. 2, except  $\omega_p = \Omega_0$ ,  $\omega_0 = 0$ ,  $k_0 = 2\Omega_0/c$  (the static helical undulator is on continuously). (a) The transverse velocity  $\beta_x$  and (b) the longitudinal displacement  $\Omega_0 \zeta_z/c$  during and after the turn-on of the probe.

electric field of the probe is canceled by the  $(\check{\zeta}_z/c)\vec{e}_z \times \vec{B}_{0\perp}$  force, which is exerted on a longitudinal plasma wave by the helical magnetic field of the undulator. The plasma wave in this example can be used for acceleration of relativistic electrons because its phase velocity is  $v_{ph} = (\omega_1 - \omega_0)/(k_1 - k_0) = -c$ .

The steady-state values of  $\beta_+ = \beta_-^* = \beta_x - i\beta_y$  and  $\zeta_z$  can be analytically obtained by a straightforward linearization of Eq. (1) in the weak probe,  $a_1 \ll a_0$ , limit:

$$\dot{\beta}_+ + i\Omega_0\beta_+ = -(\omega_0 a_0 e^{i\theta_0} + \omega_1 a_1 e^{i\theta_1} - k_0 a_0 \check{\zeta}_z e^{i\theta_0} - k_1 a_1 \check{\zeta}_z e^{i\theta_1}). \quad (4)$$

Introducing  $\theta_{0,1} = k_{0,1}z_0 - \omega_{0,1}t$  and assuming that  $k_{0,1}\zeta_z < 1$ , the exponentials in Eq. (4) are expanded, yielding

$$\dot{\beta}_+ + i\Omega_0\beta_+ = -\omega_0 a_0 e^{i\theta_0} (1 + ik_0 \zeta_z - k_0 \check{\zeta}_z / \omega_0) - \omega_1 a_1 e^{i\theta_1} (1 + ik_1 \zeta_z - k_1 \check{\zeta}_z / \omega_1). \quad (5)$$

The longitudinal equation of motion is given by

$$\check{\zeta}_z + \omega_p^2 \zeta_z \approx -\frac{e}{mc} \left( \vec{v}_\perp \times \vec{B}_\perp + \zeta_z \vec{v}_\perp \times \frac{\partial \vec{B}_\perp}{\partial z} \right),$$

where  $\vec{B}_\perp(z_0 + \zeta_z) \approx \vec{B}_\perp(z_0) + \zeta_z \partial_{z_0} \vec{B}_\perp(z_0)$ , yielding

$$\check{\zeta}_z + \omega_p^2 \zeta_z = -\frac{c^2}{2} (k_0 a_0 \beta_- e^{i\theta_0} + k_1 a_1 \beta_- e^{i\theta_1} - ik_0^2 \zeta_z \beta_- a_0 e^{i\theta_0}) + \text{c.c.} \quad (6)$$

Unlike the transverse velocity  $\beta_+$  which is excited directly by each of the two lasers according to Eq. (5), plasma waves are excited only in the presence of *two* lasers (in-

cluding the possibility of one having zero frequency) via the beatwave mechanisms.

The physical reason for the plasma transparency is the strong coupling between the longitudinal and transverse degrees of freedom of the electrons. The steady-state solution of Eq. (6),  $\check{\zeta}_z = 0.5 \check{\zeta} \exp(i\Delta k z - \Delta \omega t) + \text{c.c.}$ , where  $\Delta \omega = \omega_1 - \omega_0$  and  $\Delta k = k_1 - k_0$ , is substituted into the transverse equation of motion (5). Retaining terms with  $\exp(-i\omega_0 t)$  and  $\exp(-i\omega_1 t)$  dependence results in

$$\beta_+ = -\frac{i\omega_0 a_0}{\omega_0 - \Omega_0} e^{i\theta_0} - \frac{i\omega_1}{\omega_1 - \Omega_0} \left( a_1 + \frac{ik_0 \check{\zeta}}{2} a_0 \right) e^{i\theta_1}. \quad (7)$$

Equation (7) yields the steady-state amplitude of the plasma wave given by Eq. (3) for  $\omega_1 = \Omega_0$  and  $\Delta \omega = \omega_p$ .

The general case of  $\omega_1 \neq \Omega_0$  is handled by inserting  $\beta_+$  and  $\beta_-$  into Eq. (6):

$$(\omega_p^2 - \Delta \omega^2) \check{\zeta} = ic^2 \left[ \frac{k_0 a_0^* \omega_1}{\omega_1 - \Omega_0} (a_1 + ik_0 \check{\zeta} a_0 / 2) - \frac{k_1 a_1 \omega_0}{\omega_0 - \Omega_0} a_0^* - i \frac{k_0^2 \check{\zeta} \omega_0}{\omega_0 - \Omega_0} |a_0|^2 \right]. \quad (8)$$

Equation (8) is then solved for  $\check{\zeta}$ . Substitution of this expression for  $\check{\zeta}$  into Eq. (7) yields the steady-state perpendicular velocity:

$$\beta_{+s} = -\frac{i\omega_0 a_0}{\omega_0 - \Omega_0} e^{i\theta_0} - i \frac{\omega_1 a_1}{\omega_0 - \Omega_0} e^{i\theta_1} \frac{c^2 k_0^2 \omega_0 |a_0|^2 (k_1/k_0 - 2) + 2(\omega_p^2 - \Delta \omega^2)(\omega_0 - \Omega_0)}{c^2 k_0^2 |a_0|^2 \omega_1 + 2(\omega_p^2 - \Delta \omega^2)(\omega_1 - \Omega_0)}, \quad (9)$$

where we have neglected terms proportional to the product of the laser detuning from resonance,  $\delta \Omega = \omega_1 - \Omega_0$ , and the pump intensity  $a_0^2$ . From Eq. (9), plasma is resonantly driven when the denominator  $D = 2(\omega_p^2 - \Delta \omega^2)(\omega_1 - \Omega_0) + c^2 k_0^2 |a_0|^2 \omega_1$  vanishes. Close to cyclotron resonance,  $D \approx 4\omega_p(\Omega_R^2 - \delta \Omega^2)$ , where  $\Omega_R = ck_0 a_0 (\Omega_0 / 4\omega_p)^{1/2}$  is the effective Rabi frequency. Hence, the pump field shifts plasma resonances from  $\omega_1 = \Omega_0$  to  $\omega_1 = \Omega_0 \pm \Omega_R$ .

The fluid velocity component synchronous with the probe (i.e., proportional to  $\exp(i\theta_1)$ ) is  $b_+ \approx \beta_{+s} - \partial_z(\zeta_z \beta_{+s}) = \beta_+ - ik_1 \zeta_z \beta_+$ . Explicitly, using the results of the last paragraph,  $b_+ = ia_1 \omega_1 (\delta \Omega + \delta \Omega_0) / (\Omega_R^2 - \delta \Omega^2)$ , where  $\delta \Omega_0(k_1) = (2\Omega_R^2 \omega_0 / \omega_p \Omega_0)(k_1/k_0 - 1)$ . The expression for  $b_+$  can now be used to calculate the current in the plasma that is synchronous with the probe field. The desired dispersion relation for induced transparency in a magnetized plasma is derived from the wave equation for the probe,  $-(c^2 \partial_z^2 - \partial_t^2) \vec{E} = 4\pi \partial_z \vec{J} = -4\pi ic \omega_1 n_0 b_+ + \text{c.c.}$  One finds

$$\omega_1^2 = c^2 k_1^2 - \omega_p^2 \omega_1 \frac{\delta \Omega + \delta \Omega_0(k_1)}{\Omega_R^2 - (\delta \Omega)^2}, \quad (10)$$

where it was assumed that the frequency of the pump is fixed at  $\omega_0 = \Omega_0 - \omega_p$ . Complete transparency ( $\omega_1^2 = k_1^2 c^2$ ) is achieved at  $\omega_1 = \Omega_0 - \delta \Omega_0$ , where  $\delta \Omega_0 \approx (2\omega_0 \Omega_R^2 / \omega_p \Omega_0)(\Omega_0 / k_0 c - 1)$ . Note that this frequency shift is, in general, very small in the most interesting regime of  $\Omega_R \ll \omega_p$ :  $|\delta \Omega_0| < 4\Omega_R^2 / \omega_p \ll \Omega_R$ , and can be even smaller near cyclotron resonance when the pump and probe copropagate. Equation (10) reduces to the dispersion relation for a single probe in a magnetized plasma when the detuning is large,  $(\delta \Omega)^2 \gg \Omega_R^2$ .

Note that the index of refraction is not identically equal to unity at the cyclotron resonance. This is different from the quantum-mechanical result for a three-level system [6], where  $\omega_1 = k_1 c$  on resonance. We speculate that this difference occurs because of multiple Landau levels

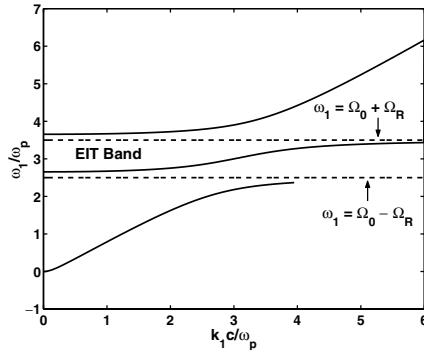


FIG. 4. EIT dispersion curve,  $\Omega_0/\omega_p = 3$  and  $\Omega_R/\omega_p = 1/2$ . Flat band above  $\Omega_0 - \Omega_R$  up to  $\Omega_0 + \Omega_R$  labeled “EIT Band” corresponds to slow light and appears only in the presence of a pump.

$E_n = n\hbar\Omega_0$  and corresponding Raman-shifted levels  $E_{Rn} = E_n + \hbar\omega_p$  which participate in the classical EIT.

The modified dispersion relation given by Eq. (10) is plotted in Fig. 4, for the same plasma parameters as in Fig. 1 and a copropagating pump with  $\Omega_R = 0.5\omega_p$ . The flat band between the  $\Omega_0 \pm \Omega_R$  resonant frequencies is a novel feature which is not present without the pump (compare with Fig. 1). The width of this transparency band, which scales as  $\Omega_R \propto a_0$ , is very narrow for low pump amplitudes. The corresponding “group velocity” (as understood in the strictly geometrical sense explained below)  $v_g = \partial\omega_1/\partial k_1 \approx 2c\Omega_R^2/\omega_p^2$  can also be made arbitrarily small. This slowly propagating wave packet of electromagnetic waves is a classical analog of the “slow light” in atomic systems [2].

Qualitatively, the spectacular slowing down of electromagnetic waves in the EIT plasma can be understood by considering the entrance of a probe beam of duration  $L_0$  into the plasma. Inside the plasma, the slow light wave packet of length  $L_f$  consists of the transversely polarized field of the probe  $|\vec{E}_1| = |\vec{B}_1| = a_1 mc\omega_1/e$  and the longitudinal electric field of the plasma wave  $E_z = 4\pi en_0(2a_1/k_0 a_0)$ . As the pulse enters the plasma, it loses photons to the pump at the same rate as new plasmons are created (according to the Manley-Rowe relations). The classical photon density of a field with frequency  $\omega$  is proportional to the action density  $\propto U/\omega$ , where  $U$  is the energy density. We calculate that the ratio of the plasmon to photon density inside the slow light pulse,

$$\frac{U_{\text{plas}}/\omega_p}{U_{\text{phot}}/\omega_1} = \frac{\Omega_0}{\omega_p} \frac{E_z^2}{2E_1^2} = \frac{\omega_p^2}{2\Omega_R^2}, \quad (11)$$

is much greater than unity if  $\Omega_R \ll \omega_p$ . Thus, most photons of the original pulse are transferred to the plasma wave. Since the refraction index remains close to unity, the photon energy density in the pulse remains roughly constant. Therefore, the loss of photons is due to the spatial shortening of the pulse from  $L_0$  to  $L_f = L_0 \times (2\Omega_R^2/\omega_p^2)$ .

Because temporal pulse duration does not change, we recover the previously calculated  $v_g/c = 2\Omega_R^2/\omega_p^2$ . It is precisely in this geometric sense of  $v_g/c = L_f/L_0$  that the group velocity of the slow light is interpreted.  $v_g$  is not related to the speed of individual photons since their number is not conserved during the pulse transition into the plasma. In the case of a static undulator, all energy is transferred to the plasma and compressed by a factor  $v_g/c$ , resulting in a dramatic increase of the energy density.

One interesting application of EIT in magnetized plasma is ion acceleration. While laser-plasma accelerators of electrons [7] have long been considered as a long-term alternative to conventional rf cavity-based linacs, the field of plasma-based ion accelerators is still in its infancy [8]. Present concepts revolve around ions generated at low energies when ultraintense lasers hit thin foils. The plasma system studied here provides a blueprint of an entirely different scheme—a short-pulse ion accelerator consisting of a slow light in the plasma with approximately equal group and phase velocities. Acceleration is accomplished by the longitudinal electric field of the plasma wave. Counterpropagating geometry could be chosen to match the phase and group velocities because  $v_{\text{ph}} = \omega_p/(|k_0| + k_1) \approx 0.5c\omega_p/\Omega_0$ . Matching  $v_{\text{ph}} = v_g$  yields  $a_0 \approx \omega_p^2/\Omega_0^2 \ll 1$ . Other accelerator concepts which rely on the ponderomotive force appear attractive because the ponderomotive force, which scales as the gradient of the energy density  $E_z^2/L_f \propto (\omega_p/\Omega_0)U_0/v_g^2$ , increases rapidly with decreasing group velocity of the probe.

This work was supported by the DOE Division of High Energy Physics and the Presidential Early Career Award for Scientists and Engineers.

*Note added.*—We became aware that a related analytic calculation was recently published in Ref. [9].

- 
- [1] K.J. Boller, A. Imamoglu, and S.E. Harris, Phys. Rev. Lett. **66**, 2593 (1991); S.E. Harris, Phys. Rev. Lett. **70**, 552 (1993).
  - [2] L. V. Hau *et al.*, Nature (London) **397**, 594 (2001).
  - [3] M. Fleischhauer, S.F. Yelin, and M.D. Lukin, Opt. Commun. **179**, 395 (2000).
  - [4] S.E. Harris, Phys. Today **7**, 36 (1997); J.P. Marangos, J. Mod. Opt. **45**, 471 (1998); A.B. Matsko *et al.*, Adv. At. Mol. Opt. Phys. **46**, 191 (2001).
  - [5] N.A. Krall and A.W. Trivelpiece, *Principles of Plasma Physics* (McGraw-Hill, New York, 1973), Chap. 4.
  - [6] M.O. Scully, Phys. Rev. Lett. **67**, 1855 (1991); M. Fleischhauer, C.H. Keitel, and M.O. Scully, Phys. Rev. A **46**, 1468 (1992).
  - [7] T. Tajima and J.M. Dawson, Phys. Rev. Lett. **43**, 267 (1979).
  - [8] R.A. Snavely *et al.*, Phys. Rev. Lett. **85**, 2945 (2000).
  - [9] A.G. Litvak and M.D. Tokman, Phys. Rev. Lett. **88**, 095003 (2002).